University of Baghdad
College of Engineering
JOURNAL OF ENGINEERING

Journal of Engineering

journal homepage: www.jcoeng.edu.iq

Volume 31 Number 10 October 2025

Optimization of Tensile Strength for Zinc- Aluminum (ZA-27/SiC) Composite Materials Fabricated by Stir Casting

Waleed T. Rashid

College of Production and Metallurgy Engineering, University of Technology, Baghdad, Iraq

ABSTRACT

One zinc-27 % aluminum alloy (ZA-27) with excellent corrosion resistance and high hardness is ZA-27, making it suitable for industrial applications such as vehicle parts. The alloy works better in tough mechanical conditions because it has carbide particles, like SiC or TiC, added to it, which make it harder, more resistant to wear, and improve its internal structure. Using Minitab statistical software, the design of experiments (DOE) was utilized to conduct studies with a statistical two-level factorial experimental design. The effect of three parameters, SiC particles percentage (X1), stirring speed (X2), and stirring time (X3), was studied on the tensile characteristics of the SiC-enhanced ZA-27. The ingot was smelted using the stir-casting process to make a composite material .Then, varied percentages of SiC particles (0 and 5 wt%), speeds (300 and 900 rpm), and stirring times (30 and 60 min.) were utilized to stir the molten metal. The regression results showed that there was a satisfactory fit of the model variability for both SiC particles (X1) and stirring speed (X2). The p-value for each parameter was less than 0.005, which is statistically significant. It was determined that the factors X1 = 5 wt%. X2 = 900 rpm, and X3 = 60 minutes could provide the greatest tensile strength of 465 MPa. The tensile strength (465.5 MPa) obtained in practice using the values of X1, X2, and X3 calculated by the programs is almost identical to that obtained practically.

Keywords: Silicon carbide particles, Stirring speed, Tensile strength, Stirring time, ZA-27 alloy.

1. INTRODUCTION

Due to their high specific strength, zinc alloys and composites exhibit far superior mechanical properties compared to pure zinc; their application is encouraged, and alloying or composites, when done properly, may offer several advantages in various applications **(Mohamed ,2023).** Previous studies have shown that, owing to the great compatibility of different Zn alloys and some alloying elements, such as Zinc-Magnesium, Zinc-Cadmium, Zn-Manganese, Zinc-Lithium, and Zn-Cerium, among others **(Fatile et al., 2017).** Traditional

*Corresponding author
Peer review under the responsibility of University of Baghdad.
https://doi.org/10.31026/j.eng.2025.10.10

Article received: 01/05/2025
Article revised: 15/07/2025
Article accepted: 23/07/2025
Article published: 01/10/2025

monolithic materials have been shown to have many challenges in achieving a suitable ratio of toughness, stiffness, strength, and elongation. To address these issues and meet the increasing need for a stronger, lighter, and more affordable material appropriate for modern engineering applications, composites have emerged as a potential material and are being chosen over traditional monolithic materials **(Moses, 2014; Arunkumar, 2018; Imtiaj et al.,2025).** Metal matrix composites (MMCs) have garnered a lot of attention in the last ten years because they provide superior mechanical and thermal properties over parent or conventional materials, including high elastic modulus, wear resistance, tensile strength, toughness, thermal stability, corrosion resistance, and strength **(Bobic et al., 2015; Arunkumar et al., 2022).** MMCs are quickly taking the place of conventional monolithic materials and metallic alloys due to their desirable properties. These applications include electronic substrates, sports facilities, automotive, aerospace, marine, and leisure industries **(Kumar et al., 2020; Saleh et al., 2024).**

Metallic alloys reinforced with harder, more durable materials are known as metal-material composites, or MMCs. While Zn, stainless steel, and Cu have also been used, light metal alloys like aluminum, magnesium, and titanium make up the bulk of metallic alloys used. Alloys made of zinc and aluminum are practical technological materials that have advantageous characteristics, including good castability, corrosion resistance, tensile strength, and tribological features **(Chen et al., 2020).** These alloys do, however, have several disadvantages, such as a high density and subpar mechanical properties at high temperatures. This, however, has been enhanced by reinforcing with ceramic particles **(Gangwar et al., 2020; Liu et al., 2022)**. **(Gurunagendra et al., 2021)** studied the stir casting technique; a study was carried out to improve ZA-27 alloys by adding fine (100 μm) zircon sand particles as reinforcement material at weight fractions of 1.5%, 3.0%, 4.5%, and 6.0%. The homogeneous dispersion of zircon particles inside the alloy matrix was confirmed by microstructural examination utilizing Energy Dispersive X-ray examination (EDAX) and Scanning Electron Microscopy (SEM). Tensile testing was used to analyze the mechanical behavior and physical characteristics, such as density and porosity. At 3.0%, 4.5%, and 6.0% reinforcing levels, the results showed a significant increase in tensile strength and yield strength, along with a decrease in ductility. The distribution of the reinforcing particles and the ensuing rise in the dislocation density inside the matrix were ascribed to this phenomenon. **(Alaneme et al., 2016)** investigated the mechanical and wear characteristics of ZA-27 composites reinforced with steel chips .The ZA-27-based composites have weight percentages of 5, 7.5, and 10 % steel. Machining chips, although unreinforced ZA-27 alloy and a composition containing 5% alumina were also created as control samples. It was observed that the hardness and wear resistance of the composites increased when the weight percentage of steel chips was increased from 5 to 10 %. But the relatively tough steel chips, not the ZA-27 matrix, were what made the steel chip-reinforced ZA-27 more fracture-tough than the unreinforced alloy and the 5 wt.% alumina-reinforced composite. **(Bhaskar et al., 2017)** studied the mechanical properties of silicon carbide-reinforced ZA-27. 0, 3, 6, and 9 weight percent SiCp were used to strengthen the ZA-27 alloy accordingly. According to reports, the ZA-27/SiCp composites' compressive strength, impact strength, tensile strength, and hardness all markedly increased as the filler content rose in comparison to the unreinforced alloy. Thus, the hard ceramic particles in the matrix alloy were thought to be responsible for this enhancement. **(Dalmis et al., 2016)** investigated the addition of graphite (Gr) nanoparticles and the mechanical and physical characteristics of ZA-27 composites. According to reports, when the amount of Gr grew, hardness and ultimate

tensile strength dropped. Because Gr particles are becoming more brittle and can quickly change the shape of the composites, using Gr in metal matrix composites is known to lower their strength in tension and compression. This happens because the Gr particles tend to clump together and have weak connections with the matrix alloy. This effect was attributed to aggregation and weak bonding between the Gr particles and the matrix alloy. The purpose of this work is to use Silicon carbide powder (SiC_P) as reinforcing particles and the stir-casting method to make a zinc matrix composite. The effects of SiC addition, stirring duration, and speed on the tensile strength of the ZA-27 alloy are investigated. Identifying the important element and impacting each element on tensile strength using the Minitab 16 application. The produced ZA-27 alloy and composite's microstructure, tensile strength, and hardness were evaluated.

2. EXPERIMENTAL WORK

2.1 Materials and experimentation

In this experiment, the matrix material is the ZA-27 alloy. **Tables 1 and 2** show the chemical composition of ZA-27 alloys and reinforcement, respectively. Where analysis was carried out using Spectro Max by the State Company for Inspection and Engineering Rehabilitation. The size of the SiC particles utilized was 30-42 µm; the particle size and volume were measured by the sieve. The vortex stir casting method and the electric furnace shown in **Fig. 1** were used to produce the composites. A mild steel impeller was used to physically spin the melt before mixing the SiC powder with the molten metal in Zn alloy. After an hour of preheating at 200°C to drive off any moisture, the particles were mixed with the agitated liquid metal **(Ali et al., 2020; Weiqi et al., 2024).** The composite was treated at a 500 rpm stirring speed and 600 °C of temperature. The melt was pumped into a steel mold at 650 °C.

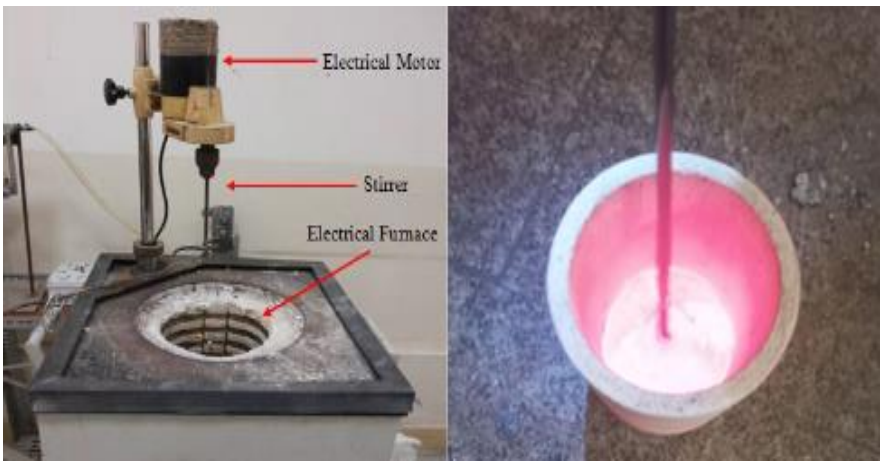

Figure 1. Stir casting technique.

Table 1. Composition of ZA-27 alloy.

Composition	Al	Cu	Cd	Fe	Mg	Zn
wt%	27	2.1	0.003	0.077	0.02	bal
Standard ZA-27	25-28	2-2.5	0.003	0.075	0.001-0.002	

Table 2. Composition of SiC.

Composition	SiC	SiO_2	Al_2O_3	Fe_2O_3	CaO	MgO
wt%	97.02	0.79	0.3	0.1	0.62	0.06

2.2 Microstructure and Hardness

The specimens were initially sliced from the center of the samples to analyze the microstructure of the base and the two produced alloys. Using the grinding equipment, three grit sizes of silicon carbide papers (320, 500, and 1000) were used for grinding. The specimens were then etched using a solution of 1.5% HCl, 1% HF, 2.5% HNO_3, and 95% water after being appropriately polished on polishing cloth with the help of 0.5 µm alumina. The resultant samples have been cleaned with alcohol and water before being dried in hot air. An optical microscope with a digital camera was used to extensively scan the microstructures of the produced alloys as well as the base alloy. Using Vickers hardness equipment, the basic alloys and the produced alloys' microhardness were measured and computed using the formula below **(Sivananthan et al., 2020).**

$$HV = 1.8544 * P / dav^2 \quad (1)$$

where:
P: The applied load is 1 Kg.
Dav: The average diameter of the rhombus indentation in (mm).
HV: Vickers hardness. Kg / mm^2.

2.3 Tensile Test

Every specimen created in this study was subjected to a tensile test in compliance with ASTM E-8 criteria **(ASTM E8M, 1991).** The test samples were machined into round specimens with a gauge length of 36 mm and a diameter of 7 mm. A 1 mm/min extension rate was used on Instron universal testing equipment, which was used for the test at room temperature. Elongation, yield strength, and ultimate tensile strength were among the tensile parameters that were assessed using the stress-strain curves that resulted from the tension testing. Three readings were taken for each specimen of the test. The tensile samples before and after the test are shown in **Fig. 2.**

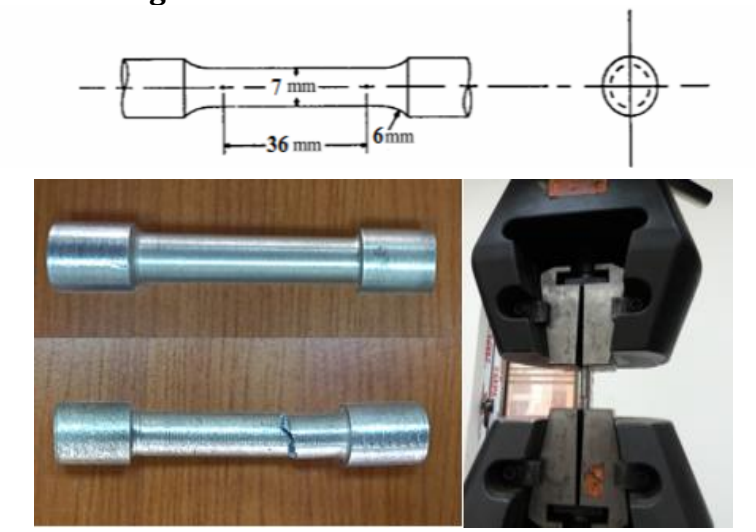

Figure 2. Samples before and after the tensile test

2.4 Full Factorial Design

This research looked at three factors: stirring time (factor X3), stirring speed (factor X2), and SiC% % (factor X1). Using a 2^3 FFD (full factorial design), the effects of these components' alterations on the tensile strength (Y) responses were assessed. Eight experimental runs were carried out in all **(Mahadevi et al., 2014; Waleed, 2024)**. Each factor's range limitations were given the values (−1) and (+1), in that order **Table 3.** Minitab 16 was used to examine the responses to the experimental design. Subsequently, the data were used in the Design of Experiments method to create mathematical models **(Padmanathan et al., 2024). Table 4** shows the factorial design's factors and levels.

Table 3. Factors and levels used in the factorial design.

Factors	X1(wt. %)	X2(rpm)	X3(min.)
Low Limit (−1)	0	300	30
High Limit (+1)	5	900	60

Table 4. Design matrix and the results of the 23 full factorial designs.

No.	X1	X2	X3	SiC wt%	Stirring speed	Stirring time	Tensile strength (Y) (Mpa)
A1	-1	-1	-1	0	300	30	410
A2	+1	-1	-1	5	300	30	428
A3	-1	+1	-1	0	900	30	425
A4	+1	+1	-1	5	900	30	459
A5	-1	-1	+1	0	300	60	418
A6	+1	-1	+1	5	300	60	440
A7	-1	+1	+1	0	900	60	431
A8	+1	+1	+1	5	900	60	465

3. RESULTS AND DISCUSSION

3.1 Microstructure and Hardness

The microstructure of the ZA-27/SiC (0 and 5 wt%) composites was examined under a light microscope. The light microscope demonstrates how the regular stirring motion produced the fine, uniform dispersion of SiC particles in the ZA-27 matrix. **Fig. 3** displays the light micrographs of the ZA-27/SiC, where the SiC percentage is 0 and 5 wt% composites. The SiC particles are shown in black areas, while the matrix is displayed in white parts. The porosity in the cast composite materials was caused by trapped air during the casting process. The zinc-aluminum matrix was treated with SiC to evaluate grain refinement; this result was confirmed by the study **(Dongxin et al., 2021). Fig. 4** displays the findings of the hardness tests conducted on the ZA-27 alloy and ZA-27/SiC. It has been shown that the hardness of the composites rises with increases in stirring duration, speed, and weight percentage of the reinforcement **(Siva and Prasanna, 2024)** represented by the codes A1 (SiC 0%, 300 rpm, and 30 minutes of stirring time) and A8 (SiC 5%, 900 rpm, and 60 minutes of stirring time). It has been discovered that the reinforcement content, stirring duration, and speed all affect the mechanical characteristics of composites. An increase in reinforcing content of up to 5%, 900 rpm of stirring speed, and 60 minutes of stirring duration led to the hardness rise from

119 to 132 Brinell Hardness (Kg/mm^2). It is anticipated that the automotive industry would benefit from this composite. This result was confirmed by the study **(Waleed and Khalid, 2021; Shivalingaiah and Nagarajaiah, 2022).**

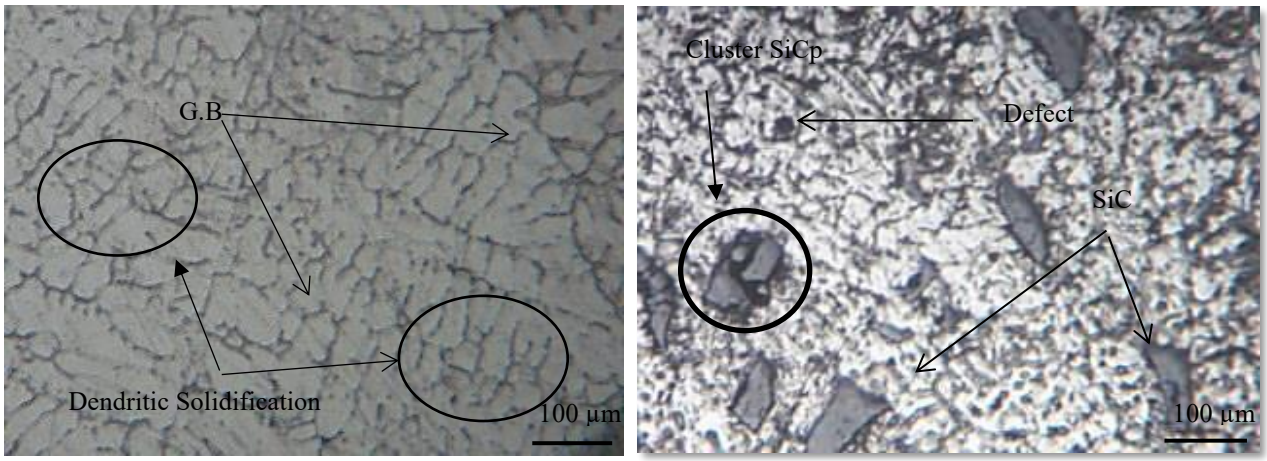

Figure 3. Light micrographs; (A) ZA-27Alloy (sample A1) and (B) ZA-27/SiC (sample A4).

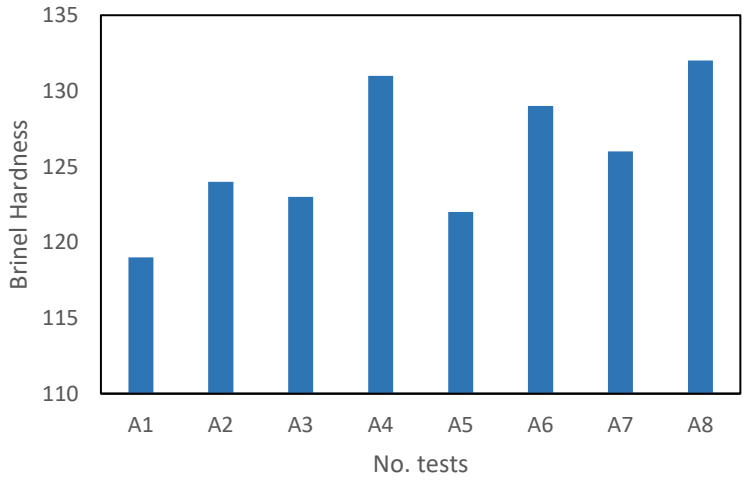

Figure 4. The hardness of ZA-27 and composites.

3.2 Statistical Analysis of Tensile Strength

The analysis was performed using MINITAB 16, a program designed especially for experiment design applications. **Table 5** presents the test circumstances and output findings utilizing 23 orthogonal arrays of full factorial design. Using a significance threshold of α = 0.05, the computed, Table 5 displays each coefficient's P-level computed. Since the coefficients with p-values larger than α = 0.05 are not significant (b3, b23), they'll be taken out of the model. The remaining coefficients are (a0, b0, b1, b2, b12, and b13). As a result, the tensile strength-derived mathematical model may be written as follows:

$$Y = 39.500 + 2.000\,X1 + 1.033\,X2 + 0.005\;X1X2 + 0.013\,X1X3 \quad (2)$$

The tensile strength is represented by (Y), and the variables stand for (X1), (X2), and (X3), respectively, the SiC%, stirring speed, and stirring duration. Equation (1) indicates that the tensile strength is most affected by the SiC% and that stirring speed (X2) has a greater impact on tensile strength than stirring duration (X3).

Table 5. Estimated regression coefficients for tensile.

Term	Regression Coefficient	Coef	SE Coef	T	P
Constant	b0	39.500	4.00000	97.625	0.000
X1	b1	2.000	0.74833	2.673	0.003
X2	b2	1.033	0.00553	6.030	0.004
X3	b3	0.367	0.08165	4.491	0.099
X1*X2	b12	0.005	0.00067	7.000	0.003
X1*X3	b13	0.013	0.01333	1.000	0.002
X2*X3	b23	-0.000	0.00011	-2.000	0.075

3.3 Analysis of Variance (ANOVA)

To separate the individual impacts from each control component, statistical design techniques such as ANOVA are used. To calculate the corresponding influence on the quality characteristic, the percentage contribution of each control component is used **(Sathish et al., 2021).** The particular wear rate-related ANOVA findings are shown in **Table 6.** At a significance level of 5% or 95% confidence level, this analysis was conducted. It is evident that although stirring speed (X2; p=0.005) has less of an impact on specific tensile strength, the SiC particle% % X1(p=0.000) has a larger effect. Finally, X3(p=0.139) indicates that the stirring speed has a greater effect than the stirring duration. With an R-sq adjusted of 99.92%, the independent variables (X1, X2, and X3) account for 99.92% of the variance found in the variable (Y), with the remaining portion being explained by additional factors like random error. The closer to one the coefficient of determination is, the better, and these can be satisfactory results.

Table 6. Specific tensile strength for ANOVA

Source	DF	Seq SS	Adj SS	Adj MS	F	P
Regression	6	2576.00	2576.00	429.333	214.67	0.000
Linear	3	2468.00	79.19	26.396	13.20	0.003
Interaction	3	108.00	108.00	36.000	18.00	0.171
Residual Error	1	2.00	2.00	2.00		
Total	7	2578.00				
S = 1.4142		R-Sq = 99.92%			R-Sq(adj) = 99.46%	

3.4 Main Effect Plot of Tensile Strength

Fig. 5 illustrates that the effect of stirring time, speed, and SiC% affects tensile strength. It is observed that when stirring duration, speed, and SiC% % increase, the tensile strength progressively rises. The excellent dispersion of SiC particles in the matrix alloy with increasing weight fractions is responsible for the observed steady rise in tensile strength with increasing weight fractions. The elongation percentage of ZA-27 metal matrix composites decreased as the material became tougher and SiC quantities increased, the

result is agreed with **(Nithin et al., 2024).** The tensile strength of the composite material will rise in tandem with the increase in the hardness of the basic ZA-27 alloy due to the contribution of the SiC particles' hardness **(Waleed, 2023).** During the tensile test, the matrix's restriction to plastic deformation increases when stiffer and harder SiC reinforcement particles are present. The increased tensile strength value is unmistakable proof that the inclusion of particles in the matrix has raised the composites' overall hardness **(Kumar and Tirth, 2013; Simsek et al., 2020).** The effect of the stirring speed was positive on increased tensile strength, which is caused by the high stirring speed resulting in the dispersion of reinforcing particles in the alloy matrix, which enhances the tensile strength. This result was confirmed by the study **(Singh et al., 2013; Uday and Rajamurugan, 2022).** The tensile strength of the ZA-27/SiC composite rises with longer stirring times, which gives the reinforcement particles enough time to diffuse into the matrix **(Kheradmand and Tayebi, 2022).**

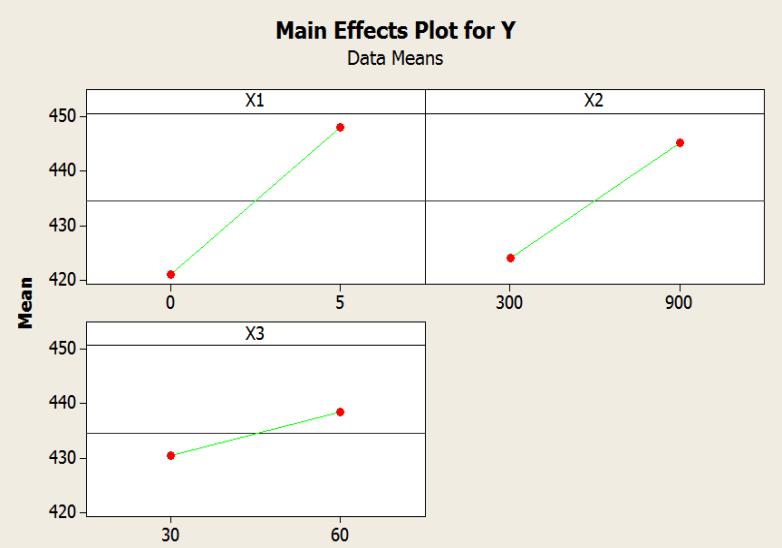

Figure 5. Main effect plot of residuals of tensile strength

3.5 Response Surface Analysis

The plots of response surface primary goal are to identify the ideal operating parameters, which are expressed as the SiC%, stirring speed, and stirring time, and which ultimately result in the needed maximum tensile strength. The plots are three-dimensional, and the contours show the effects of variables. (X1, X2, and X3) On a response (Y) are shown in **Fig. 6 A, B, and C**. Tensile strength increases are shown by the proportion of SiC particles, stirring speed, and stirring duration in three-dimensional and contour plots. It is noteworthy that the percentage of SiC particles has a bigger influence on the tension resistance than stirring speed; that is, tensile strength rises dramatically with increasing SiC particle percentage **(Liu et al., 2022).** On the other hand, you'll see that stirring.

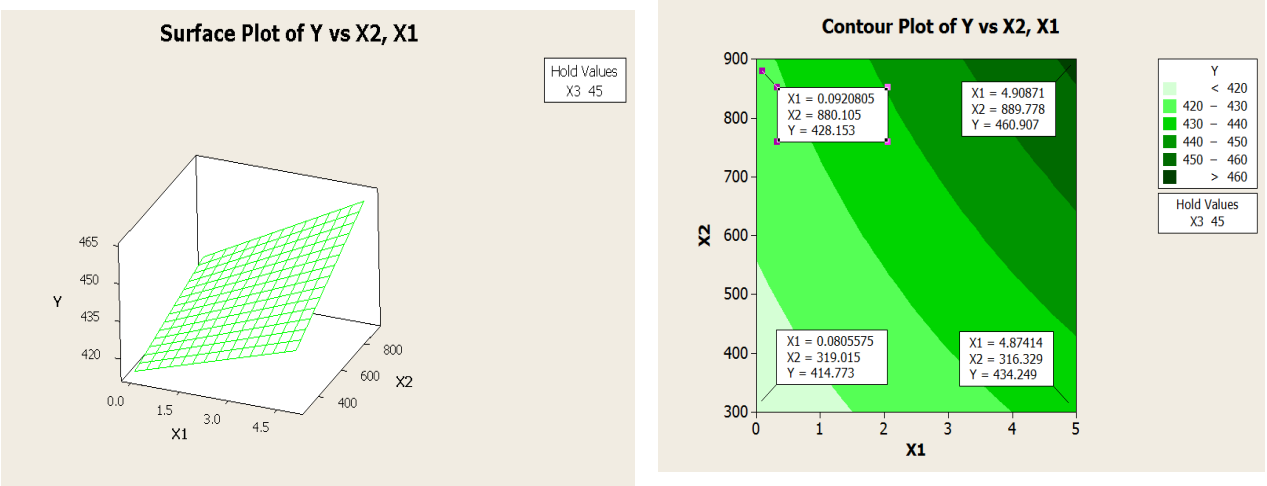

A. Three-dimensional and Contour plot of tensile strength, effects of X1, and X2 on a response (Y).

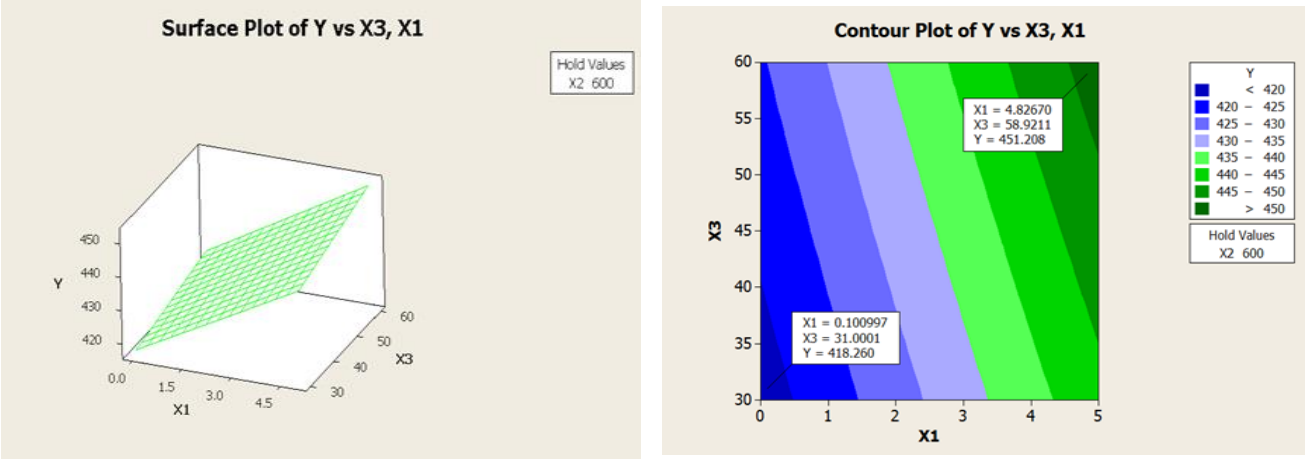

B. Three-dimensional and Contour plot of tensile strength, effects of variables X3 and X1 on a response (Y).

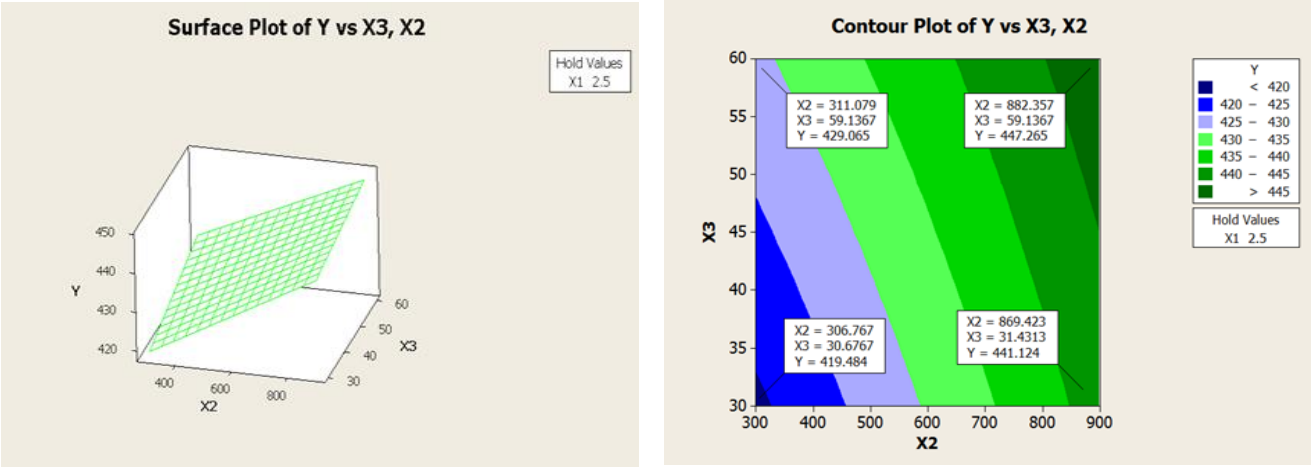

C. Three-dimensional and Contour plot of tensile strength, effects of variables X3 and X2 on a response (Y).

Figure 6. Three-dimensional and Contour plot of tensile strength, effects of variables X1, X2, and X3 on a response (Y).

3.6 Interaction Plot of Tensile Strength

To illustrate the link between a continuous response and a single categorical component, used an interaction plot. **Fig. 7** shows the interaction effects of the control parameters. It is often known that when lines on interaction plots are parallel, no interaction occurs, and when lines cross or are italicized, considerable interaction tends to occur between factors **(Fnides, 2012; Venkatesan and Anthony, 2018). Fig. 7** analysis of the tensile strength reveals a significant interaction between the control parameters. It was observed that a SiC particle has the greatest effect on tensile strength, while stirring time has the weakest effect on tensile strength. The best result, according to the graph, can be obtained at a high value of rotational speed and a high value of SiC particles. The findings show that the SiC particle-containing samples have greater yield and tensile strengths than the base alloy. Furthermore, the strength of the composites increases as the particle content does, just as the micro-hardness attribute. According to the Orowan curvature, the alloy's resistance is related to the grain-displacement interaction **(Chebolu et al., 2022).** When residual displacement rings remain surrounding each grain after the dislocation passes through the particles, the material's strength increases. The interaction between dislocations and non-shear particles increases the strength of composite materials. The presence of SiC particles affects the tensile strength of all composites. As per the Orowan mechanism, the SiC particles function as barriers, impeding the dislocations from moving in proximity to the reinforcing particles within the matrix **(Krishnan et al., 2020; Mussatto et al., 2021)**. High rotational speed generates the highest tensile stress value is at the 900rpm rotational speed. This shows that the filler adhered well to the matrix at a screw speed variation of 900 rpm. The increase in the rotational speed rises in particle dispersion in the matrix of the composite.

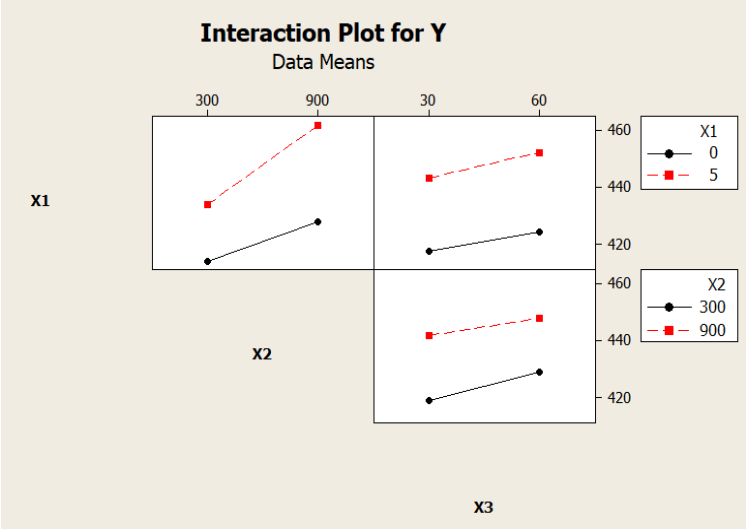

Figure 7. Interaction plot of tensile strength.

3.7 Optimization of Tensile Strength

The tensile strength optimization chart for the two components at different values (X1, X2, and X3) is shown in **Fig. 8.** The left column displays the optimization result, and the center of the top row displays each parameter's ideal setting. Each factor's behavior curve is shown below. An ideal run at SiC percentage (5 wt%), stirring speed (900 rpm), and stirring

duration (60 min.) is predicted by the chart to produce a tensile strength of (465.5 Mpa), which is almost identical to that produced by the program.

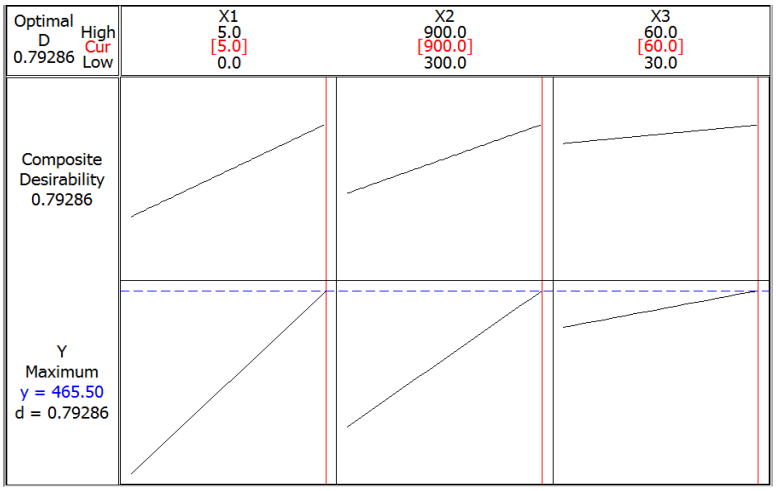

Figure 8. Optimization chart for maximum tensile strength.

4. CONCLUSIONS

In this study, using the stir-casting technique, the zinc matrix composite containing SiC reinforcement particles was fabricated successfully. It is found that the tensile strength increases with the increase of SiC particle proportion, stirring speed, and stirring time. This might be because the particles' distribution in the matrix became more uniform. The optimum tensile strength (465 MPa) was reached at SiC particle percentage (X1:5 w%), stirring speed (X2:900 rpm), and stirring time (X3:60 min.). When using these factors, values of X1, X2, and X3 apply to the programs, the best tensile strength (465.5 MPa) that can be achieved, and this result is close to the results that have been practically accomplished. However, the tensile strength is significantly impacted by X1 and X2. As for X1, it has the most effect. As for hardness, increased reinforcing content of up to 5%, 900 rpm of stirring speed, and 60 minutes of stirring duration led to the hardness rising from 119 to 132 BH (Kg/mm^2).

Credit Authorship Contribution Statement

Waleed T. Rashid: Conceptualization, Methodology, Investigation, Data curation, Formal analysis, Writing – original draft, Writing – review & editing, Visualization, Supervision, Project administration.

Declaration of Competing Interest

The author declares that he has no known competing financial interests or personal relationships that could have appeared to influence the work reported in this paper.

REFERENCES

Arunkumar, K. N., Krishnappa, G. B., 2022. Mechanical properties of aluminum metal matrix composites - a review. *International Journal of Engineering Research and Technology (IJERT)*. 11, pp. 174-178. https://doi.org/10.17577/IJERTV11IS030111.

Arunkumar, K. N., Krishnappa, G.B., Kasturirengan, S., Laxman, B.R., 2018. An experimental investigation on the hardness and shear behavior of aluminum, silicon carbide, and graphite hybrid composite with and without cryogenic treatment. *Materials Today: Proceedings*, 5, pp. 916–921. http://doi.org/10.1016 /j.matpr. 2017.11.163.

Alaneme, K.,K, Adeoye, K.,O., Oke, S.,K., 2016. Mechanical and wear behavior of steel chips reinforced Zn27Al composites. *Leonardo Electronic Journal of Practices and Technologies (LEJPT).* .29, pp. 1–16.

Ali, M., Arab, A., 2020. Review of stir casting technique and technical challenges for ceramic reinforcement particulate and aluminum matrix composites. *Journal of Silicate-Based and Composite Materials.* 72(6), pp.198-204. http://doi.org/10.14382/epitoanyag-jsbcm.2020.32.

ASTM E 8M, 1991. Standard test method for tension testing of metallic materials (metric), Annual Book of ASTM Standards, Philadelphia.

Bobic, B., Bobic, I., A., Vencl, M., Babic, Mitrovic, S., 2015. Corrosion behavior of compo casted ZA-27/SiCp composites in NaCl solution. *Tribol in Ind* .38(1), pp. 67-72.

Bhaskar, R., Hemanth, C., Jayasimha, N., 2017. Mechanical characterization of ZA-27 reinforced with SiCp MMCs. *Third International Conference on Current Trends in Engineering Science and Technology (ICCTEST)*, pp. 232-237.

Chen, F., Binbin W., Zhiqiang C., 2020. Microstructure and wear behavior of in situ ZA27/TiB_2 Composites. *Metals*. 10(12),1663, pp.2-17. https://doi.org/10.3390/met10121663

Chebolu, R., Nallu, R., Chanamala, R., 2022. Influence of SiC/TiB_2 particles addition on corrosion behavior of as-cast Zn-Al-Cu alloy hybrid composites. *Hindawi, Journal of Eng*ineering. 2022, pp 1–5. http://doi.org/10.1155/2022/3669584.

Dlmis R., H., Cuv, l., A., Kci, C., Gul, O., R.,.2016. Investigation of Graphite nano particle addition on the physical and mechanical properties of ZA27 composites. *Advanced Composites Letters*,25(2), pp. 37-42. https://doi.org/10.1177/096369351602500202.

Dongxin, M., Xiangchen, M., Yuming, X., Yuchen, Y., Yanli, X., Zhiwei, Q., Yuexin, C., Long, W., Yongxian, H.,2021. Strength-ductility balance strategy in SiC reinforced aluminum matrix composites via deformation-driven metallurgy. *Journal of Alloys and Compounds.* 891(25). http://doi.org/10.10 16/j.jallc om.2021 .16 2078

Fatile, B., O., Adewuyi, B., O., Owoyemi, H., T., 2017. Synthesis and characterization of ZA-27 alloy matrix composites reinforced with zinc oxide nanoparticles. *Engineering Science and Technology*. pp. 1147-1154. http://dx.doi.org/10.10 16/j.jestch. 2017.0 1.001

Fnides, B., 2012. Analysis of technological parameters through response surface methodology in machining hardened X38CrMoV5-1 using whisker ceramic tool (Al_2O_3+SiC). *Estonian Journal of Engineering*. 18(1), pp. 26–41. http://doi.org/10.3176/eng.2012.1.03.

Gangwar, S., Payak, V., Pathak, K., Jamwal, A., Gupta, P., 2020. Characterization of mechanical and tribological properties of graphite and alumina reinforced zinc alloy (ZA-27) hybrid metal matrix composites, *Sage Journal*, 54, pp. 4889–4901.

Gurunagendra, R., Raju, R., Vijayakumar, P., Amith, G., H Hanumantharaju, G., Santosh A.,2021. Investigations on microstructure and tensile properties of as-cast ZA-27 metal matrix composite reinforced with zircon sand. *Materials Today: Proceedings*, 46(17), pp. 7618-7623.

Imtiaj, H., Minhaz, A., Tafsirul, H., 2025. An experimental study on the mechanical properties of stir-cast hybrid Al metal matrix composite reinforced with Al_2O_3 and TiO_2. *Journal of Engineering Advancements*. 6(1), pp. 1-10. https://doi.org/10.38032/jea.2025.01.001

Kumar, G.B., Gouda, P.S., Pramod, R., Chowdary, U.S., Subash, T., Vamsi, M.S., Naresh, K., 2020. Development and experimental evaluation of titanium diboride particulate reinforcements on the Al6061 alloy composites' properties. *Advanced Materials Process. Technol*. 8, pp. 1209–1225. http://doi.org/10.1080/23740 68X.2020.1855399

Kumar, P., Tirth, V., 2013. Effect of stirring speed on retention of particles in AA2218-A1203 metal matrix composite processed by stir casting. *MIT International Journal of Mechanical Engineering*. 3(2), pp. 123-128.

Kheradmand, A.B., Tayebi, M., Z., 2022. Lalegani design of Fe–SiC–Cu–G composite alloy and optimization of graphite contribution for high sliding speed applications. *Transactions of the Indian Institute of Metals* .75(9), pp. 2311–2322. http://doi.org/10. 100 7/s12666-022-02562-0.

Krishnan, P., Arunachalam, R., Husain, A., 2020. Studies on the influence of stirrer blade design on the microstructure and mechanical properties of a novel aluminum metal matrix composite. *Journal of Manufacturing Science and Engineering*. 143(2), pp. 1–25. http://doi.org/10.1115/1.4048266

Liu, K., Jiang, X., Chen, S., Yuan, T., Yan, Z., 2022. Effect of SiC addition on microstructure and properties of Al–Mg alloy fabricated by powder and wire cold metal transfer process. *journal of materials research and technology*. 17, pp. 310-319. https://doi.org/10.1016/j.jmrt.2022.01.014.

Liu, Y., Du, T. , Qiao, A. , Mu, Y., Yang, H., 2022. Zinc-based biodegradable materials for orthopaedic internal fixation. *Journal Funct Biomater*. 13(4), 164, pp. 1-20. http://doi.org/10.3390/jfb13040164

Mohamed, K. D., Mohamed, K., K., 2023. Tensile and compressive mechanical properties of ZA27/ molybdenum disulfide, metal matrix composite. *Research Engineering Structure Materials*. 9 (3), pp. 709-718. http://dx.doi.org/10.17515/resm2022.583me1112

Moses, J., Dinaharan, I., Joseph, S., 2014. Characterization of silicon carbide particulate reinforced AA6061 aluminum alloy composites produced via stir casting. *Procedia Materials Science*. 5, pp. 106 – 112. http://dx.doi.org/10.1016/j.mspro.2014.07.247

Mahadevi, D., Manikandan, M., 2014. Modelling and parametric optimization using factorial design approach of TIG welding of AZ61 magnesium alloy. *SSRG International Journal of Mechanical Engineering (SSRG-IJME).* 1, pp. 16-20. http://doi.org/10.14445/23488360/IJME-V1I1P104

Mussatto, A., Ahad, I., Mousavian, T., 2021. Advanced production routes for metal matrix composites. *Engineering Reports. John Wiley and Sons Inc*.3(5), pp. 1-25. http://doi.org/10. 1002/eng2.12330.

Nithin, B., N., Nagaral, M., Maiyya, M., Nalband F., Auradi, V.,2024. Mechanical properties of ZrO_2 particles reinforced Al2219 alloy metal composites prepared by the stir casting process. *Journal of Mines, Metals and Fuels.* 72(9), pp. 937-947. http://doi.org/10.18311/jmmf/2024/45198

Padmanathan, P., Aswin, S., Satheesh, A., Kanna, P.R., Palani, K., Devi, N.R., Sobota, T., Taler, D., Taler, J., and Węglowski, B., 2024. Parametric Optimization Study of Novel Winglets for Transonic Aircraft Wings. *Applied Sciences (2076-3417)*, *14*(17), P. 7483. https://doi.org/10.3390/app14177483

Saleh, B., Fathi, R., Radhika, N., Yu, Z., Liu, S., Zhang, L., 2024. Effect of yttrium oxide on microstructure and mechanical properties of functionally graded magnesium matrix composites. *Journal of Alloys and Compounds*. 981, P. 173723.

Sivananthan S., Ravi K., Samson C. J., 2020. Effect of SiC particle reinforcement on the mechanical properties of aluminium 6061 alloy processed using the stir casting route. *Materials Today: Proceedings,* 21(1), pp. 968-970. http://doi.org/10.1016/j.matpr.2019.09.068

Siva, R. M., Prasanna, P., 2024. Optimisation of friction spectral process parameters on AA8011 reinforced with titanium dioxide (Tib_2) and zirconium oxide (ZrO_2). Metal hybrid matrix. *International Journal of Mechanical Engineering and Technology (IJMET).* 15, pp. 9-25.

Shivalingaiah, K., Nagarajaiah, V., 2022. Stir casting process analysis and optimization for better properties in Al-MWCNT-GR-based hybrid composites. *Metals* 12, 1297, pp. 1-25. http://doi.org/10.3390/met12081297.

Sinatora, A., Viafara. C., 2009. Influence of hardness of the harder body on wear regime transition in a sliding pair of steels. *Wear*. 267(1), pp. 425-432. http://doi.org/10. 1016 /j.wear.2008.11.019.

Sathish, T., Mohanavel, V., Arunkumar, T., Raja, T., Rashedi, A., Alarifi, I. I., Badruddin, A., Algahtani, Afzal, A., 2021. Investigation of mechanical properties and salt spray corrosion test parameters optimization for AA8079 with reinforcement of TiN + ZrO_2. *Materials (Basel).*4(18). https://doi.org/10.3390/ma14185260.

Simsek, D., Simsek, I., Ozyurek, D., 2020. Relationship between Al_2O_3 content and wear behavior of Al+2% graphite matrix composites. *Sci Eng Compos Mater*. 27, pp. 177–185. http://doi.org/10.1515/secm-2020-0017

Singh, L., Ram, B., Singh, A., 2013. Optimization of process parameters for stir casted aluminum metal matrix composite using the Taguchi method. IJRET. *International Journal of Research in Engineering and Technology*. 2(8), pp. 357-383. http://doi.org/10.15623/ijret.2013.0208059

Uday, K., Rajamurugan, G.,2022. Effect of stir casting parameters and mono/hybrid reinforcements on aluminium metal matrix composite-A review. *Institution Mechanical Engineering. Part C Journal.* 236, pp. 4904–4920. http://doi.org/10.1177/ 09544062211052166

Venkatesan, S., Anthony, M. X., 2018. Tensile behavior of aluminum alloy (AA7050) metal matrix composite reinforced with graphene fabricated by stir and squeeze cast processes. *Science and Technology of Materials* .30, pp. 74–85. http://doi.org/10.10 16/j.st mat.2 018.02.005.

Waleed, R., 2024. Optimization of wear resistance of aluminum matrix composite (Al-7050/10wt% eggshell) by study of effect stirring speed and stirring time. *Kufa Journal of Engineering*. 15(4), pp. 83-97. http://doi.org/10.2423 7/djes . 2016.09108

Waleed, R., 2023. Mechanical properties characterization of Al 7075 / phosphogypsum metal matrix composites. *Kufa Journal of Engineering.* 14 (1), pp. 67-80. https://doi.org/10.30572/2018/KJE/140105.

Waleed, R., Khalid, R., 2021. Improvement and optimization of the hardness for the aluminum metal matrix composite using eggshell. *Materials Science Forum.* 1039, pp. 42-50. https://doi.org/10.4028/www.scientific.net/MSF.1039.42.

Weiqi, Y., Mohommad, R. M., Pawan, K., Matthew, A. W., Frank, E., Roger H. F., 2024. Exploring 2D X-ray diffraction phase fraction analysis with convolutional neural networks: Insights from kinematic-diffraction simulations. *MRS Advances,* 9, pp.921–928. http://doi.org/10.15 57/s4 3580-024-00862-9

تحسين قوة الشد للمواد المركبة ZA−27/SiC المصنعة بطريقة الصب بالتحريك

وليد تركي راشد

كلية هندسة الإنتاج والمعادن ,الجامعة التكنولوجية,بغداد,العراق

الخلاصة

سبيكة الزنك والألومنيوم ZA-27 هي سبيكة تتميز بمقاومة ممتازة للتآكل وصلابة عالية، مما يجعلها مناسبة للتطبيقات الصناعية مثل قطع غيار السيارات. تعمل هذه السبيكة بشكل أفضل في الظروف الميكانيكية القاسية بفضل إضافة جزيئات الكربيد، مثل SiC أو TiC، مما يجعلها أكثر صلابة ومقاومة للتآكل، ويحسن بنيتها الداخلية. باستخدام برنامج Minitab الإحصائي، استُخدم تصميم التجربة (DOE) لإجراء دراسات بتصميم تجريبي إحصائي عاملي ثنائي المستوى. دُرس تأثير ثلاث معاملات، وهي نسبة جسيمات كربيد السيليكون (X1)، وسرعة التحريك (X2)، وزمن التحريك (X3)، على خصائص الشد لـ ZA-27 المُحسَّن بكربيد السيليكون. صُهرت السبيكة باستخدام عملية الصب بالتحريك لصنع مادة مركبة. بعد ذلك، استُخدمت نسب متفاوتة من جسيمات كربيد السيليكون (0 و5%)، وسرعات دوران (300 و900 دورة في الدقيقة)، وأزمنة تحريك (30 و60 دقيقة) لتحريك المعدن المنصهر. أظهرت نتائج الانحدار توافقًيا مُرضيًا لتباين النموذج لكلٍ من جسيمات كربيد السيليكون (X1) وسرعة التحريك (X2). كانت القيمة الاحتمالية لكل معامل أقل من 0.005، وهي دلالة إحصائية. تَبيّن أن العوامل X1 = 5wt%، و X2 = 900 rpm، وX3 = 60min.، تُوفِّر أقصى مقاومة شد قدرها 465 ميجا باسكال. وتُعَدُّ مقاومة الشد (465.5 ميجا باسكال) المُكتسبة عمليًا باستخدام قيم،X1 X2, X3 مُتطابقة تقريبًا مع تلك المُستقاة من البرنامج.

الكلمات المفتاحية: دقائق كربيد السليكون، سرعة الخلط، مقاومة الشد، زمن الخلط، سبيكة زنك− 27 المنيوم.